A Study on Application of Dielectric Resonator Antenna in Implantable Medical Devices

(Article begins on next page)

13 May 2024

A Study on Application of Dielectric Resonator Antenna in Implantable Medical Devices

SUMER SINGH SINGHWAL[1,2], (Member, IEEE), **LADISLAU MATEKOVITS**[2,3,4], (Senior Member, IEEE), **ILDIKO PETER**[5], AND **BINOD KUMAR KANAUJIA**[6], (Senior Member, IEEE)

[1]Department of Electronics and Communication Engineering, Chandigarh University, Chandigarh 140413, India
[2]Dipartimento di Elettronica e Telecomunicazioni, Politecnico di Torino, 10129 Torino, Italy
[3]Instituto di Elettronica e di Ingegneria dell'Informazione e delle Telecomunicazioni, National Research Council of Italy, 10129 Turin, Italy
[4]Department of Measurements and Optical Electronics, Politehnica University Timisoara, Politehnica University, 060042 Timisoara, Romania
[5]Department of Engineering and Information Technology, "George Emil Palade" University of Medicine, Pharmacy, Science, and Technology of Târgu Mures, 540088 Târgu Mures, Romania
[6]School of Computational and Integrative Science, Jawaharlal Nehru University, Delhi 110067, India

Corresponding author: Ildiko Peter (ildiko.peter@umfst.ro)

ABSTRACT Worldwide, a large number of patients are benefited every year due to technological advancement in implantable medical devices (IMDs) such as in hyperthermia and bio-telemetry. The combination of sensors and antennas defined the quality of the implantable device. Antenna communities strive hard to fulfill the needs of the medical world by introducing new designs and concepts in this field. The purpose of this study is to identify major existing challenges and provide suitable solution of these challenges for implant applications. Present implant antennas have faced inferior performance due to high metallic losses and varied implant depth. The human body is a combination of dielectric materials, regardless of whether it is liquid (eg. water), gels or hard bones. In this study, first time a dielectric resonator antenna (DRA) resonating at 2.45 GHz, has been proposed as an implantable antenna with no metallic losses, varied implant depth performance and bio-compatibility. The implant DRA is placed on a bio-compatible polyvinyl chloride (PVC) substrate with a thickness of 0.5 mm. The rectangular DRA excited by a coplanar waveguide feed is proposed and its performance is compared with the help of four phantoms given in the literature. A detailed link design study was also undertaken in view of the different applications.

INDEX TERMS Dielectric resonator antenna (DRA), implant antennas, link design, SAR.

I. INTRODUCTION

Active Implantable Medical Devices (IMD) such as cochlear implants, haemodynamic support, implantable cardiac pacemakers, implantable defibrillators and implantable glucose monitors are procured by ambulatory centers, cardiac centers, dental clinics and hospitals for their patients. These are important devices that are responsible for biotelemetry: biomedical communication, transfer of physiological information including hyperthermia, blood details, cardiac beat and other such data which can be further used for timely treatment of present or future diseases in the body. Sensors and radiators are essential components of any IMD. In rare cases, the antenna can also act as a sensor because the quality of the signal strength at a fixed link distance can convey

The associate editor coordinating the review of this manuscript and approving it for publication was Chua Chin Heng Matthew.

information about physiological data such as tissue density in cancer disease. Designing an implant antenna faces multiple challenges such as, miniaturization, efficient link budget, frequency detuning, corrosion, and displacement due to the aging of the body and the changing environment around the transmitter. Although initial research is more focused on the simplest single skin model, deeply implanted antennas considering fat and muscle are also needed. It is obvious that a deeper implant antenna will face greater challenges owing to the complex structure and composition of muscles in different parts of the body. In recent times the application of IMDs has increased significantly because of their life support. Research on wireless IMDs and other implantable sensors has increased over the last decade. The requirement of an efficient wireless communication link between On/Off body devices leads to the challenge of designing an optimum implantable antenna. The shift from the medical implant
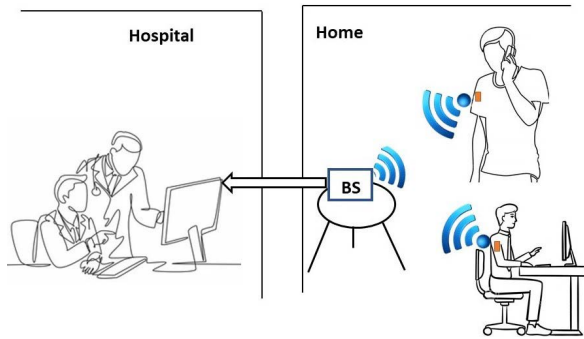
FIGURE 1. Concept of 'doctor at home'.

communication service (MICS) band (402-405 MHz) to industrial, scientific and medical (ISM) band (902-928 MHz and 2400-2483.5 MHz) is understandable due to the higher gain and possible miniaturization of implantable antennas.

Different design considerations regarding implantable antennas have been discussed in [2]–[9]. Ingestible antennas [10]–[14] and ISM band implantable antennas [15]–[25] have also been discussed for diagnostics and monitoring purposes. These implantable antennas also strengthen the concept of 'doctor at home' as illustrated in Fig. 1, wherein patient can do 'work from home', while doctor can examine the reports sent by the 'human arm implanted transmitter' through the base station available at home.

A. MOTIVATION

Microstrip patch antennas are currently only solution for ingestible and implantable body antennas because of their various advantages, such as low profile and easy miniaturization. The human body is a combination of dielectric and conductive materials as shown in Table-1 [1]. Therefore, designing a metallic patch antenna for this lossy environment may become a tedious task but using a dielectric as a resonator in this high-permittivity environment may be a better choice. In the future, it may be possible that the human body which is a dielectric body, can act as a resonator as well as a radiator with all safety measures. Owing to the absence of metallic losses and high gain with design flexibility, DRA overcomes the disadvantages of microstrip patch antennas. Miniaturization is also possible in DRA if high permittivity biocompatible dielectric material like TiO_2, Al_2O_3 are chosen. In addition, in the case of a semi-artificial limb replacement surgical scenario, implantable DRA can easily be customized according to the structural conditions. In this study, a futuristic implantable dielectric resonator antenna is proposed. To the author's knowledge, no other implantable DRA work has been reported in the literature. In this study, the design steps for implantable DRA and a simple rectangular DRA (RDRA) with coplanar waveguide (CPW) feed are presented. For an in-depth study, four phantoms were used to demonstrate the performance of the proposed RDRA. These phantoms are rectangular single-layer skin models, a rectangular three-layer (skin-fat-muscle) model, improved

TABLE 1. Dielectric properties of human tissues at 2.45 GHz [1].

Human Tissue	Dielectric constant (ϵ_r)	Conductivity (σ (S/m))	Loss Tangent ($\tan \delta$)
Skin	38.06	1.4410	0.2835
Muscle	52.79	1.705	0.2419
Fat	5.285	0.1023	0.1450
Cortical Bone	11.38	0.3943	0.2542

cylindrical three-layer model and a 3D canonical right arm tissue model in ANSYS HFSS ® EM simulator. To strengthen the study bio-compatibility and specific absorption rate analyses have also been provided. A link design study is also a very important part of the implanted antennas. An efficient path loss model for in-body to off-body communications in the ISM band was discussed in [26]. Various biomedical applications differ on the basis of data rate, transmitter power and link distance for example, saturation of peripheral oxygen (SpO_2), blood pressure or electrocardiogram (ECG) may require a data rate as low as 100 Kbps and on the contrary, multi-channel electroencephalogram (EEG) sensors or capsule endoscopes may require a 1.5 Mbps data rate [27]. For any biomedical application, a significant data rate and link distance are prominent characteristics to ensure that discriminative information is delivered within an acceptable time frame for the most critical scenario. This study demonstrates that DRA can be used in biomedical applications. In the future we may see 'human body-like material' based 'gel-DRA' which may easily adapt and perform harmlessly and efficiently in the lossy and harsh environment of the human body.

The remainder of this paper is organized as follows: Introduction section discusses the need and motivation for this study; the second section explains the manual and algorithm based methodology to design an implantable DRA and provides insight into bio-compatibility issues in implant antennas; the next section discusses radiation mechanism in four different phantoms and study implant DRA with the help of simulated result analysis including evaluation of radiation pattern, gain, impedance bandwidth, and specific absorption rate; the next section briefly discusses the link budget analysis for the proposed DRA; followed by conclusions and references.

II. DESIGN METHODOLOGY

A. DRA MODEL

Implantable antennas have a wide range of applications such as IMDs (pacemaker, defibrillators etc.), ingestible capsules (for endoscopy, intestinal diagnostics etc.), hyperthermia, cancer detection and other biotelemetry applications. After aiming for the application and operating frequency (f_0), a DRA can be designed considering the following points:

1. DRA height and substrate thickness should be minimum to achieve miniaturization,;
2. Biocompatible materials may be used for DRA, and substrate or biocompatible material coating may be used
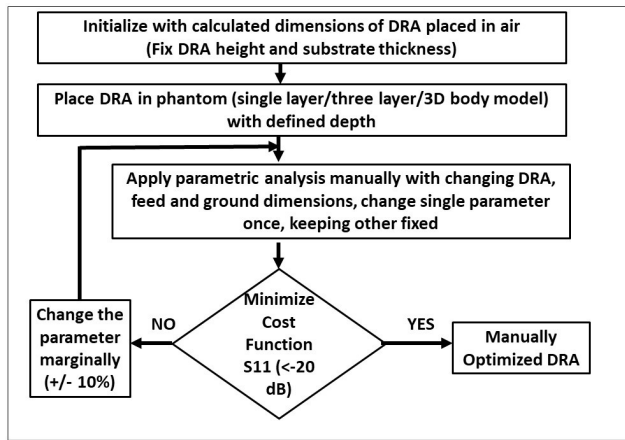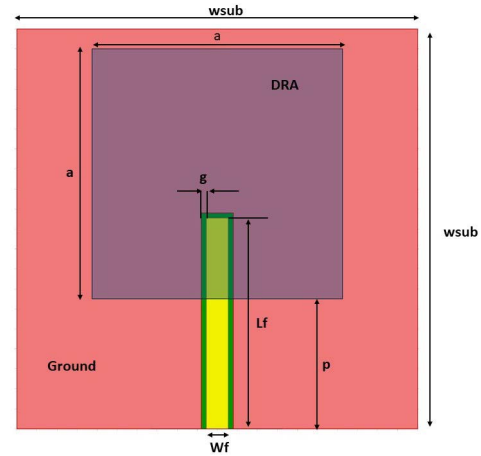
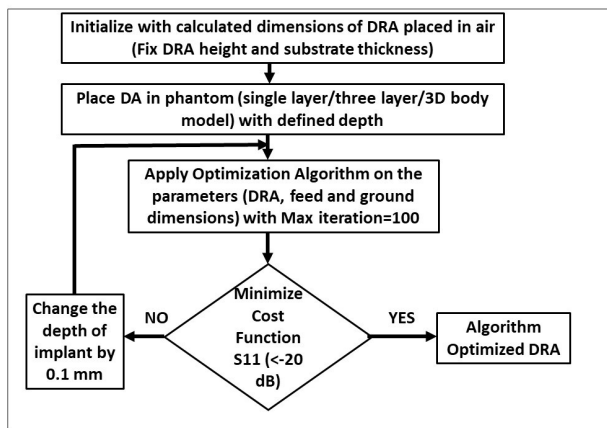**FIGURE 2.** Manually optimized Implantable DRA.

FIGURE 3. Algorithm optimized Implantable DRA.

on the substrate and DRA as the antennas are to be implanted inside the body,;

3. Excitation methodology, such as probe feed, microstrip line feed, aperture couple feed, and coplanar waveguide feed, must be chosen, considering the internal body environment and maximum power limitation with respect of RF exposure and specific absorption rate values as per international standards.

Ceramics (eg. TiO_2, Al_2O_3), Hydroxyapatite (HA), Tricalcium phosphate (TCP), polymers and polymer/ceramic composite materials are widely used in various biomedical applications [32], [33], [35]–[38]. Bio-compatible blends based on polyvinylchloride (PVC) and natural polymers can also be used in medical device fabrication [33]. Mostly, DRA are made up of biocompatible ceramics which are widely used in Periodontology and Implant Dentistry [39], [40]. These ceramics have already proven safe for human body. In this study a cuboid DRA made up of ceramic of TiO_2 with ϵ_r=80 is placed on PVC plastic substrate with ϵ_r=2.7 of thickness 0.5 mm. The approximate dimensions of the DRA were calculated using Marcatili's approximation method [46]–[48] at 2.45 GHz for the $TE_{11\delta}$ mode

FIGURE 4. Geometry of the proposed antenna.

given by Eq.(1-4).

$$k_x = \pi/a; \quad k_y = \pi/b \tag{1}$$

$$k_z tan(k_z d/2) = \sqrt{((\epsilon_r - 1)k_o^2 - k_z^2)} \tag{2}$$

$$k_x^2 + k_y^2 + k_z^2 = \epsilon_r k_o^2 \tag{3}$$

$$k_o = (2\pi f_o)/c \tag{4}$$

where, k_x, k_y, k_z denotes wavenumbers along x, y, z directions, respectively. k_o denotes free space wavenumber corresponding to resonant frequency f_o and a, b, d are length, breadth and height of rectangular DRA for relative dielectric constant range of $10<\epsilon_r<100$. To avoid the ground plane at the bottom side of the substrate which can lead to losses and high power requirements to achieve desired results inside the body environment, a coplanar waveguide feed is used to excite RDRA. In implant antennas, the dimensions of the device play an important role; therefore thickness of the substrate is fixed at 0.5 mm and the height of the RDRA is also locked at 5 mm. The dimension of DRA are compact 23.5 mm × 23.5mm × 5 mm which can be accomodated in implantable devices easily. It is made up of biocompatible ceramic so it weigh less which made it suitable for implant applications. The overall thickness of the DRA and substrate is 5.5 mm which is much less than that of previously published implantable antennas with physical dimensions of ($62\times 35\times 7.8$ mm^3) and ($54\times 31\times 11$ mm^3) in [49] and [50], respectively. Hence, we believe that physical size of the discussed implantable DRA is fit for limb muscle implantation. In Fig. 2 and Fig. 3 two design methodology are shown to design the DRA for implantable applications. These are manually parametery-based optimization and advanced algorithm-based optimization of DRA. There are different advanced optimization algorithms that are responsible for minimizing the cost function provided to them. These are genetic algoritm (GA), quasi-newton, pattern search, sequential gradient, different variants of particle swarm optimization (PSO). Both the methods are efficient but in our case algorithm-based optimization consumes more time, as it took

TABLE 2. Design parameters.

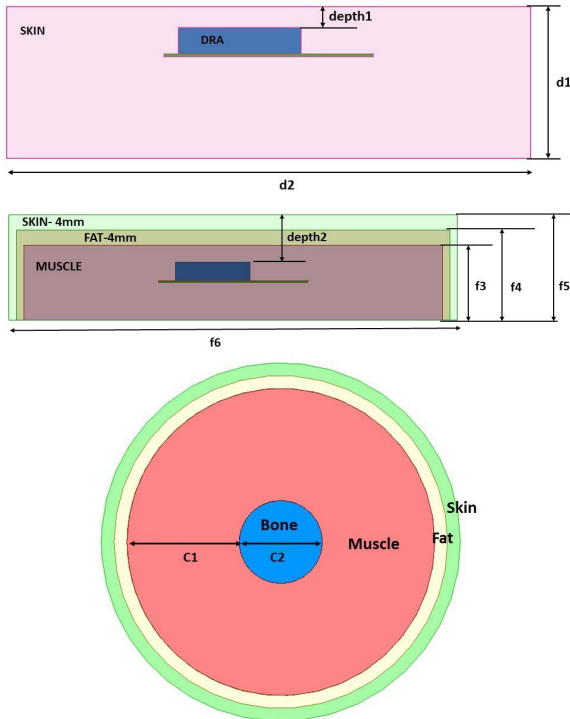| Parameter	in mm	Parameter	in mm
wsub	40	p	13.75
Lf	25.3	Wf	2.2
a	23.5	g	0.5
Thickness of substrate	0.5	height of DRA	5

FIGURE 5. Rectangular single layer (skin) model M-1 (Top), Rectangular three-layer (skin-fat-muscle) model M-2 (Middle), Cylindrical three-layer (skin-fat-muscle) model M-3 (Bottom).

approximately 2 h 45 min to complete one iteration in the 3D canonical right arm tissue model in ANSYS HFSS® Electromagnetic simulator using a computer with an Intel® i7 (2.4 GHz) processor, 16 GB RAM and 4 GB graphics card. Therefore, the manual optimization methodology mentioned in Fig. 2 has been adopted here to achieve optimized dimensions of DRA. Four phantoms were used in this study:

1. The rectangular single-layer skin model (M-1) mentioned in [2], [7], [11], [17]–[19] with d1=30 mm and d2=100 mm;
2. The rectangular three-layer (skin-fat-muscle) model (M-2) mentioned in [2], [7], [11], [17]–[19] with f3=12 mm and f6=100 mm, fat and skin thickness 4 mm each,;
3. The cylindrical three-layer (skin-fat-muscle) model (M-3) with c1=35 mm c2=26 mm, fat and skin thickness 4 mm each; M-1, M-2 and M-3 are shown in Fig. 5;
4. 3D canonical right arm tissue model (in HFSS EM simulator) as shown in Fig. 6.

B. SPECIFIC ABSORPTION RATE (SAR)

Electromagnetic waves emitted by wireless devices should not cause medical concerns for users. To asses potential risks from electromagnetic waves, a safety parameter
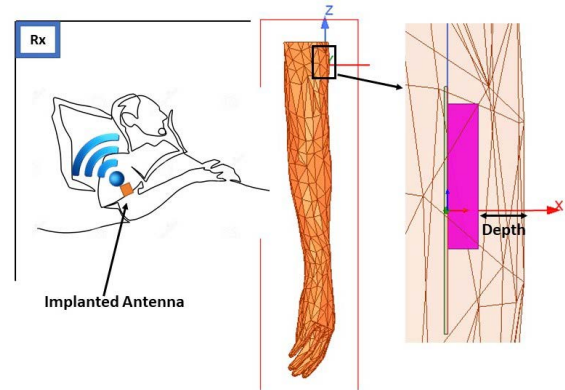

FIGURE 6. 3D canonical right arm tissue model in HFSS.

TABLE 3. Simulated SAR and maximum allowed input power of the proposed antenna.

Maximum SAR (W/Kg) values for Input Power of 1W	
1-g avg	388.38
10-g avg	53.97
Maximum allowed net Input Power (mW)	
IEEE C95.1-1999	2.25
IEEE C95.1-2005	37

known as SAR is adopted by international agencies which is defined as ''The time derivative of the incremental energy (dW) absorbed by (dissipated in) an incremental mass (dm) contained in a volume element (dV) of given density (ρ). It is expressed in units of watts per kilogram (W/kg)'' [28]. The IEEE C95.1-1999 standard restricts the SAR averaged over any 1 g of tissue to be less than 1.6 W/kg [28], and the IEEE C95.1-2005 SAR averaged over any 10 g of the tissue be less than 2 W/kg [29].Therefore, standard C95.1-1999 is stricter than standard C95.1-2005. In recent guidelines [30] whole-body average SAR was taken in tune with the International Commission on Non-Ionizing Radiation Protection (ICNIRP) guidelines [31] for frequencies above 10 MHz are 10 W/m². Table-3 showcase the different SAR values with respect to two standards (C95.1-1999 and C95.1-2005) for the 1 W input power. To abide by the SAR limits, the maximum allowed net input power should be confined to the values in Table-3. The maximum value of the SAR field is 388.38 W/kg and 53.97 W/Kg for 1-g avg and 10-g avg cases respectively, and maximum allowed net input power of both cases, calculated by simulated implant antenna model in human arm phantom by decreasing the input power to reach the international standard limits, are given in Table-3. It is confirmed from tabulated data that maximum allowed net input power for both the standard are 2.25 mW and 37 mW which are more than required when input power is less than 1 mW provided by internal battery.

C. BIO-COMPATIBILITY

One of the major concerns faced by, implant antenna engineers is bio-compatibility. Generally, a superstrate dielectric layer of Teflon (ϵ_r=2.1, tan δ=0.001), alumina ceramic (ϵ_r=9.4-9.8, tan δ=0.006) and MACOR®(ϵ_r=6.1,

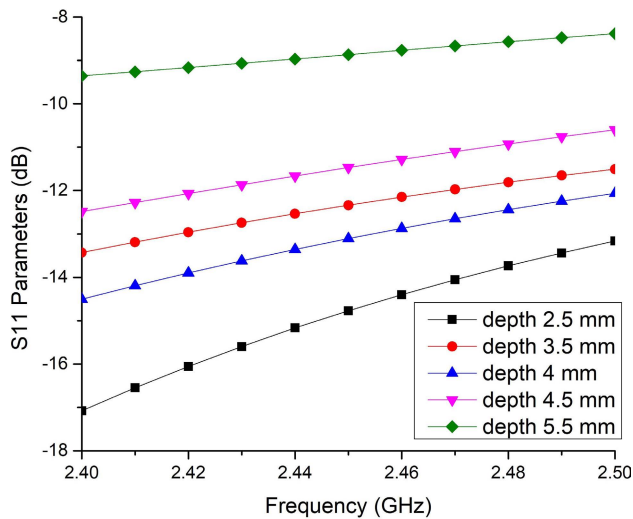**FIGURE 7.** S_{11} parameters of RDRA in rectangular single layer skin model.

FIGURE 8. Interpretation of radiation in rectangular single layer skin model.

FIGURE 9. Simulated gain of RDRA in rectangular single layer skin model M-1 at 2.45 GHz and $\phi = 0$.

tan δ=0.005) is used to preserve the bio-compatibility of the antenna. Another technique to achieve bio-compatibility in implant antennas is the introduction of a thin layer around 0.05 mm, of low loss coating of materials such as zirconia (ϵ_r=29, tan $\delta \simeq$0), PEEK (ϵ_r=3.2, tan δ=0.01) and silastic MDX-4210 (ϵ_r=3.3, tan $\delta \simeq$0) biomedical grade base elastometer [3], [34]. Zirconia is preferred by designers because of its high permittivity and low loss tangent which allow the near field of the implanted radiator to concentrate inside the encapsulation layers and to reduce power loss [35].

III. DRA RADIATION MECHANISM AND RESULT ANALYSIS

In this study, the behavior and patterns of implanted DRA inside the human body were studied by using an electromagnetic simulator have been studied. A rectangular single-layer skin model as shown in Fig. 5, was adopted for implanting the DRA. It is a well established fact that the human body is a lossy dielectric one, so it was interesting to see the S-parameter variation of a given DRA in a rectangular single-layer skin model comprising skin tissues with electrical parameters, as shown in Table 1. The depth of the implanted DRA inside this model has been varied in practical permissible limits (depending upon human body anatomy) and its effect is shown in Fig. 7. This indicates that as the depth increases, impedance matching deteriorates which indicates a trade-off between both. However, in this case orientation fluctuation was ignored to reach a conclusion. It can be seen that the 'depth of implanted DRA' introduces a gap of 'moderate dielectric constant medium' called skin which provides a smooth transition of dielectric medium, from high-permittivity (DRA) to low-permittivity medium (air). Because this inserted medium is also lossy with high tan δ therefore it attenuates the radiation. Therefore, the DRA may show proper impedance matching in this '*depth window*' (depth=2.5-4.5 mm) where tradeoff between smooth
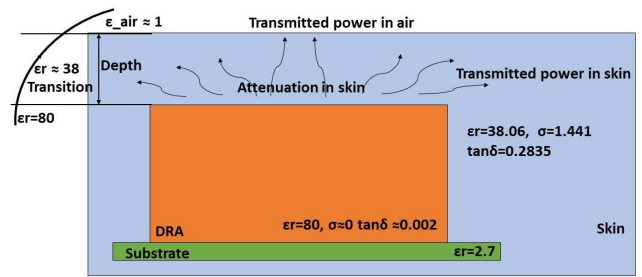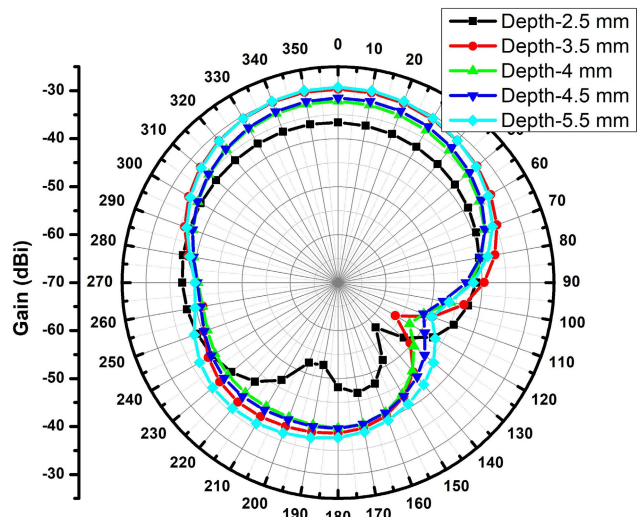
transition and attenuation, both provided by the skin layer hold in favor. In [51], Snell's law was used to describe the radiation mechanism of the implanted antenna which also holds good here, because varied dielectric mediums involved in the body and electromagnetic waves undergo refraction under these conditions which causes the spread of electromagnetic energy in a denser medium and hence attenuation of wave. Figure 9 shows the simulated gain variation at 2.45 GHz, $\phi = 0$, for different depths of the implanted DRA in the single-layer model. The gain of the implanted antenna in the broadside direction (at $\theta = 0$ and $\phi = 0$) varies from −36 dB to −29 dB moving deeper inside the skin in the suitable '*depth window*' defined earlier.

In the literature, three-layer model with skin-fat-muscle was used to justify the performance of the antenna in approximate body conditions by including three human tissues as shown in Fig. 5 [2], [11], [17], [18]. The S_{11} parameters for different implant antenna depths inside three-layer model are shown in Fig. 10. It represents that as implant antenna depth increases, impedance matching deteriorates, similar to single-layer model case. But here the useful '*depth window*' (depth=4.5-10 mm) is fairly large. Figure 11 shows the interpretation of the radiation mechanism in a three-layer model.
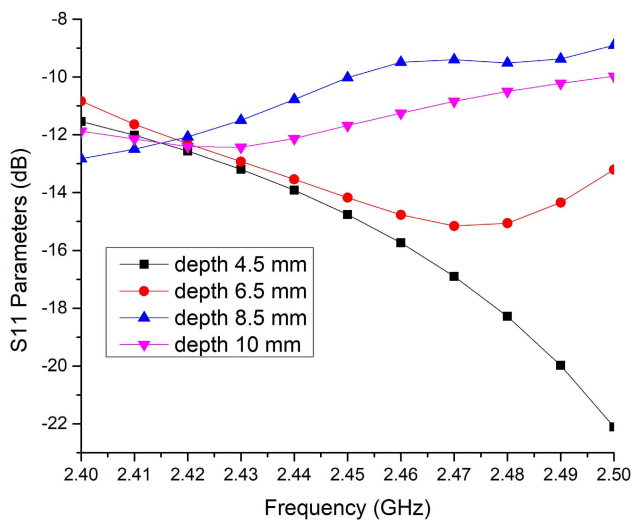
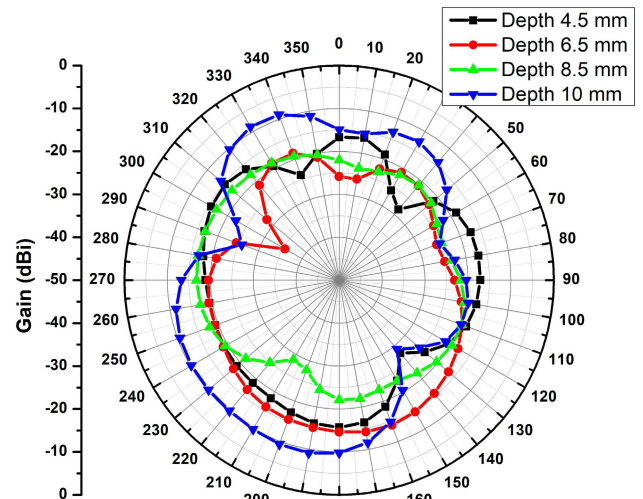**FIGURE 10.** S_{11} Parameters of RDRA in rectangular three layer model.

FIGURE 12. Simulated gain of RDRA in rectangular three layer model M-2 at 2.45 GHz and $\phi = 0$.
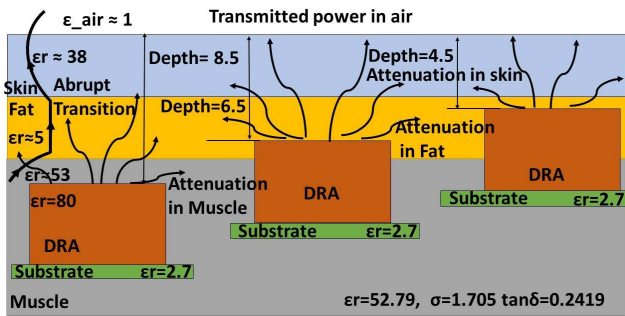

FIGURE 11. Interpretation of radiation in rectangular three layer model.

FIGURE 13. S_{11} Parameters of RDRA in Cylindrical three layer model.

This indicates that as the depth of the implanted antenna increases, the dielectric constant of different media causes abrupt transition which results a loss of signal and poor impedance matching. Figure 12 shows the simulated gain variation at 2.45 GHz, $\phi = 0$ for different implant antenna depths. It depicts that the gain in the broadside direction varies from −14.9 dB to −25 dB for the 'depth window' in the three-layer model case. It is also observed from Fig. 12 that, as the depth increases radiation from transmission line dominates more due to impedance mismatch.

The two previous phantom models discussed were rectangular in nature whereas the human arm was round shaped. Therefore, to increase similarities with the natural human arm, a rectangular three-layer model was modified to a cylindrical shape, keeping all three layers (skin-fat-muscle) along with bone, as shown in Fig. 5. Table-1 has been referred to the electrical properties of skin, fat, muscle and bone. Parametric analysis of S_{11} and gain at 2.45 GHz and $\phi = 0$ are shown in Fig. 13 and 14 with respect to the depth of the implant antenna which varies from 13 mm to 4 mm. It is observed that for lower depths, impedance matching and gain are good, but as the implant antenna moves inside the model impedance matching deteriorates. Broadside gain varies from −8.88 dBi
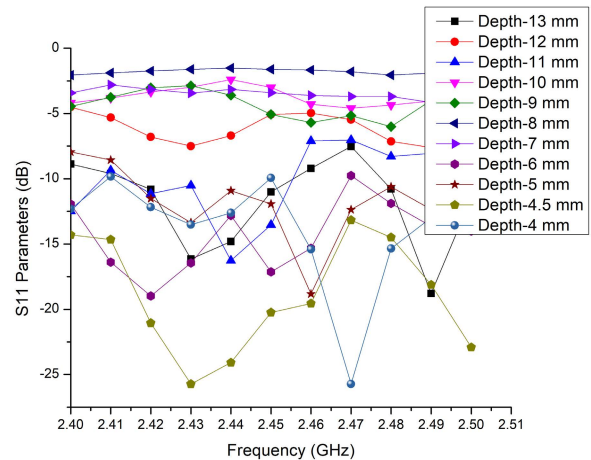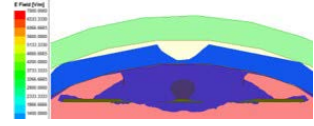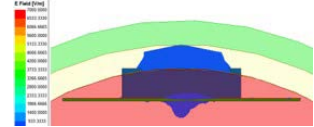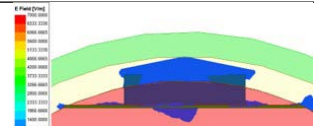
to −29.47 dBi as shown in Fig. 14. At depth=4.5 mm best impedance matching is observed throughout the operating band, and the simulated gain is −14.02 dB. It is also observed from Fig. 14 that, back radiation from the transmission line dominates more due to impedance mismatch, as the depth of the implant increases. Figure 15 shows radiation mechanism in the cylindrical model, and it is observed that as the depth decreases, the curvature effect of the cylindrical model becomes stronger. Table-4 shows the electric field distribution in the cylindrical model for the four implant depths. This shows that electric field is trapped between two high-permittivity mediums, that is skin and muscle, which results in the loss of radiation. It is also essential to mention that effective wavelength (λ_{eff}) varies with the medium and λ_{eff} for skin, fat and muscle is calculated as 19.85 mm, 53.26 mm and 16.85 mm, respectively, from $\lambda_{eff} = \lambda_0/\sqrt{\epsilon_r}$ where λ_0 is wavelength in air or vacuum. Similar to the previous models (M-1 and M-2), here, a 'depth window' (depth=4 mm-7 mm) is found in which the implant antenna performs satisfactorily.

TABLE 4. Electric field distribution in cylindrical three layer model M-3.

Depth (mm)	E.F. Distribution
9	
8	
7	
6	
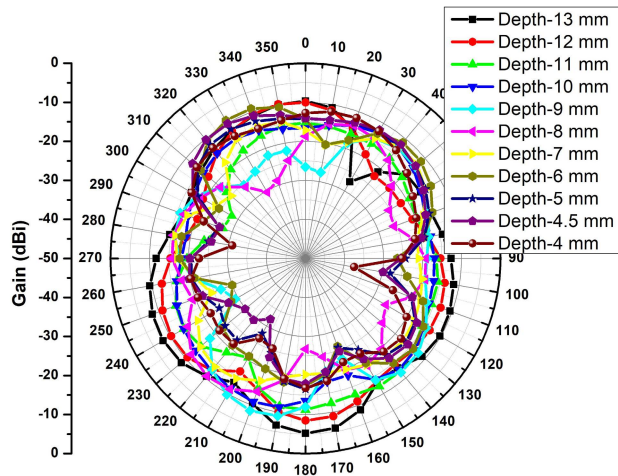
FIGURE 14. Simulated gain of RDRA in Cylindrical three layer model at 2.45 GHz and $\phi = 0$.

Finally, a simulation analysis was performed on the 3D canonical right arm tissue model using commercially available full-wave FEM based Ansys HFSS (v19.3) software in the frequency domain. Far-field distance for the proposed antenna at 2.45 GHz frequency is approximately 25 mm (equivalent to $\lambda_0/5$). The antenna characteristics have been measured at a distance of 50 cm from the skin of human arm model which lies in far-field region. Due to smaller mesh size for more accurate results complete human body with anatomical arm could not be simulated in an available 16 GB RAM, i7 processor (2.4 GHz) machine, which force us to take smaller body part. So, the upper human arm was chosen because it has thick muscle and fat, which resembles the chest and thighs, but the optimization time taken by the EM solver effectively reduced as compared to the complete human torso. But the critical dense mesh size ensures the
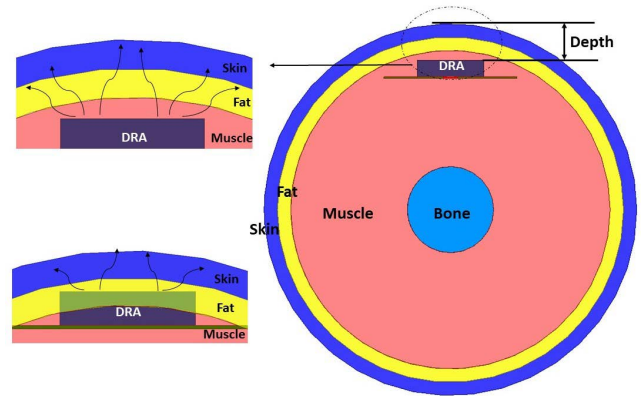
FIGURE 15. Interpretation of radiation in cylindrical three layer skin model M-3.

accuracy of results similar to human body. Simulation has been performed on both sexes human arm model (of adult person) and only male body results are displayed, as very less deviation in the results has been observed in both the cases. S_{11} parameters and simulated gain at 2.45 GHz, $\phi = 0$ are shown in Fig. 16 and Fig. 17 for different implant antenna depths. Owing to the asymmetric construction of the human body and variable dielectric constant, the S_{11} parameter varies instantly for different depths, but it makes a '*depth window*' (depth=2.3-5 mm) for which the impedance bandwidth is under -10 dB in the band of interest. As expected gain drops and varies from -23.6 dBi to -29.5 dBi for different implant antenna depth in the '*depth window*' in broadside direction (here at $\theta = 90$ and $\phi = 0$) due to change in inclination of human arm model in the HFSS solver. To verify the results obtained from HFSS solver which is based on finite element method (FEM) technique, the proposed implant DRA has been simulated on CST solver which is based on finite-difference time-domain (FDTD) technique, for different types of phantoms and a impedance bandwidth comparison of both the solvers has been displayed in Fig. 18 for depth 4.5 mm. Various results obtained from both the solvers comply mutually and confirm the performance of implant DRA.

IV. LINK BUDGET ANALYSIS

In this section, a generalized link budget analysis is undertaken in view of different applications for which implanted antennas have been proposed. EIRP, or effective isotropically radiated power, or equivalent isotropically radiated power, is a measurement of output power in one direction from an ideal, one-dimensional source. The ideal point-source radiates electromagnetic energy in a spherical pattern, so the ''maximum'' radiated power should be the same in all directions. In link design theory, the EIRP is represented by Eq. (5).

$$EIRP(dB) = P_t + G_t - L_{feed} \qquad (5)$$

P_t, G_t, and L_{feed} are transmitter power, the transmitter antenna gain, and feeding loss, respectively.
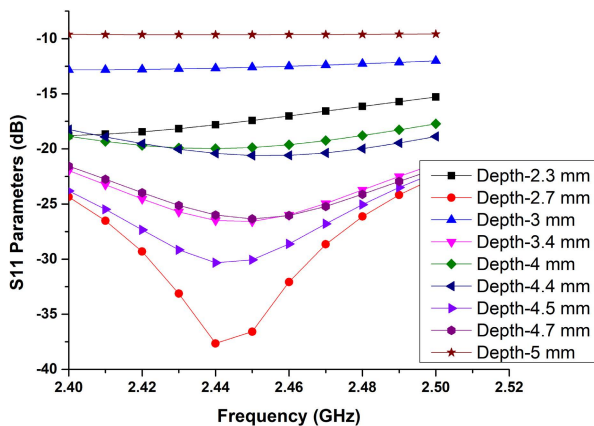
FIGURE 16. S_{11} Parameters of RDRA in 3D canonical right arm tissue model in HFSS.
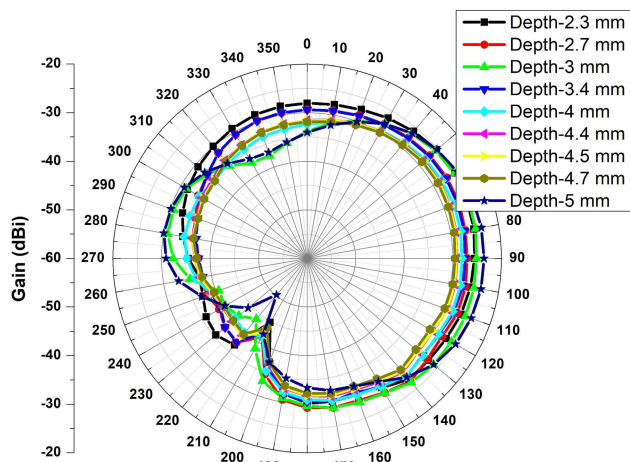

FIGURE 17. Simulated gain of RDRA in 3D canonical right arm tissue model in HFSS at 2.45 GHz and $\phi = 0$, here broadside is $\theta = 90^o$ for Human Arm Model.

Dipole antennas are assumed to be well matched, so their impedance mismatch losses are negligible. Polarization mismatch losses were also neglected. The impedance mismatch loss is represented by Eq. (6) and for S_{11}=−10 dB, −15 dB, −20 dB, the impedance mismatch losses are calculated as 0.458 dB, 0.14 dB and 0.044 dB, respectively, which can be neglected in link design.

$$L_{imp}(dB) = -10\,log_{10}\big(1 - |\Gamma|^2\big) \qquad (6)$$

where $|\Gamma|$ is magnitude of the reflection coefficient.

Free space path loss is an important factor in link design and is represented by Eq.(7). Here, the implant antenna depth inside the human body is neglected compared to the distance of the external receiver antenna. Therefore, the medium between the implanted antenna and receiver antenna is assumed to be free space. Therefore, it is important to consider the factor because the wireless independence and power of the transmitter depend primarily on the optimum distance between the links. For a body worn or nearby located external antenna in the room of the patient, distance may be
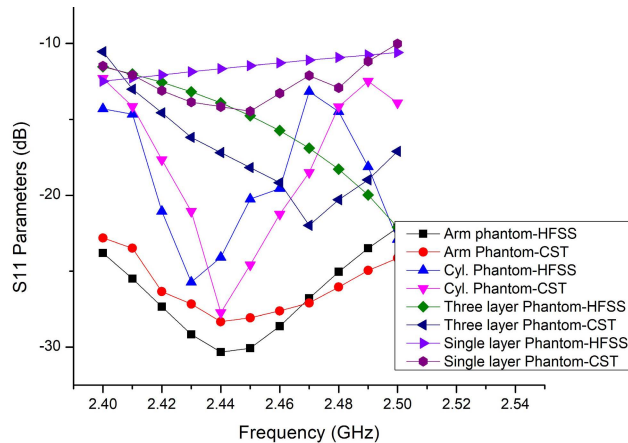

FIGURE 18. Comparison between HFSS and CST simulated S_{11} Parameters for depth 4.5 mm in different phantoms.

TABLE 5. Different transmit power and bit rates as per the biomedical application.

Reference	Transmitter Power of Implant Antenna P_t (dBm)	Bit Rate B_r (kbps)
[11]	-4	$5 X 10^3$
[13]	-10	$1 X 10^3$
[14]	-4	$78 X 10^3$
[17], [25]	-40	7

compromised for a lower value, say $d < 5$ m.

$$L_f = 20log_{10}\Big(\frac{4\pi d}{\lambda}\Big) \qquad (7)$$

At the receiver, the noise power density N_0 depends on the noise factor (NF) as shown in Eq. (8) and Eq. (9), this NF is taken as 2.5 or 3.5 depending upon the dipole antenna used. The ambient temperature (T_0) of the receiver also affects the value of the noise power density which is generally taken as room temperature (293 K).

$$N_0 = 10log_{10}(k) + 10log_{10}\big(T_i\big)\,(dB/Hz) \qquad (8)$$
$$T_i = T_0(NF - 1)\,(K) \qquad (9)$$

To design a feasible link, the margin between the required C_R/N_0 and the current link C/N_0 should be non-negative. Link C/N_0, required C_R/N_0 and link margin (LM) are described by Eq. (10), Eq. (11) and Eq. (12), respectively.

$$Link\;C/N_0 = EIRP - L_t + G_r - N_0\;(dB/Hz) \qquad (10)$$
$$Required\;C_R/N_0 = E_b/N_0 + 10log_{10}(B_r)$$
$$- G_c + G_d\;(dB/Hz)$$
$$\qquad (11)$$
$$LM(dB) = Link\;C/N_0 - Required\;C_R/N_0 \qquad (12)$$
$$LM(dB) = P_t + G_t - L_{feed} - L_t + G_r - N_0$$
$$- \big[E_b/N_0 + 10log_{10}(B_r) - G_c + G_d\big]$$
$$\qquad (13)$$

Equation (13) shows that LM depends heavily on the transmitter power (P_t), bit data rate (B_r) and distance (d) between the transmitter and receiver (in free-space path loss).
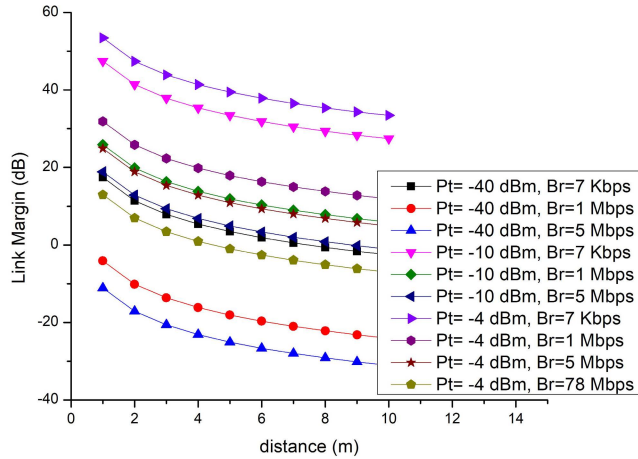
FIGURE 19. Link margin with respect to distance between transmitter and receiver antenna for best case scenario when antenna gain is −23.6 dB for 3D canonical right arm tissue model.

The transmitter power largely depends on the allowable maximum power limits in accordance with the SAR standards. The bit data rate depends on the biomedical application; for example, blood pressure, heart rate, blood oxygen and glucose monitoring require a maximum data rate of 40-200 samples/second. In biomedical applications, higher data rates are preferable to reduce latency and ensure timely delivery of critical biomedical data to health professionals. However, higher data rates can be sacrificed in some applications to manage power efficiency at larger link distances.

A. LINK BUDGET PARAMETERS FOR PROPOSED RECTANGULAR DRA

In this section, only one case of the 3D human arm model is used to calculate the link budget parameter of proposed RDRA out of the number of cases and models discussed. However, in biomedical applications, different link budget parameters can also be calculated. Using Eq. (5-12), the link design parameters were calculated for 25 μW (−16 dBm) transmitter power and are listed in Table 6. In this case, LM was found to be positive, which emphasizes the feasibility of the link setup for discussed implant DRA. It has been observed that researchers used different sets of transmitter power and bit data rates to transfer the signal from the transmitter to the receiver, in the implant antenna wireless link design, as shown in Table 5.

To better understand the effect of the transmit power and bit data rate on the performance of the antenna, various values of LM have been calculated for different link distances, transmit powers and bit data rates given in Table-5. Figure 19 and 20 show the variation of LM for the best (−23.6 dB) and worst (−29.5 dB) antenna gains in the 3D human right arm case. It can be observed from Fig. 19 and 20, that, the proposed RDRA can be utilized for different biomedical applications under ubiquitous circumstances.

TABLE 6. Link budget parameters and calculations.

Transmitter (Implant)	
Frequency (GHz)	2.45
Tx Power P_t (dBm)	-16.02
Tx Power P_t (dBW)	-46.02
Tx Power P_t (W)	25×10^{-6}
Tx Antenna Gain G_t (dBi)	-23.6
Feeding Loss L_{feed} (dB)	1.0
EIRP (dBW)	-70.62
Propagation	
Distance d (m)	5
Free Space Path Loss L_f (dB)	54.21
Air Propagation Loss L_a (dB)	0.5
Total Propagation Loss L_t (dB)	54.71
Receiver	
Rx Antenna Gain G_r (dBi)	2.15
Ambient Temperature T_0 (K)	293
Boltzmann Constant k (JK^{-1})	1.38×10^{-23}
Receiver Noise Factor (NF) (dB)	2.5
Feeding Loss L_{feed} (dB)	1.0
Noise Power Density N_0 (dB/Hz)	-202.17
Signal Quality	
Bit Rate B_r (Mbps)	1
Bit Error Rate (BER)	1×10^{-5}
E_b/N_0 (Ideal PSK) dB	9.6
Coding Gain G_c	0
Fixing deterioration G_d	2.5
Calculated Results-Link Budget	
Link C/N_0 (dB/Hz)	77.98
Required C_R/N_0 (dB/Hz)	72.1
Link Margin (dB)	5.88
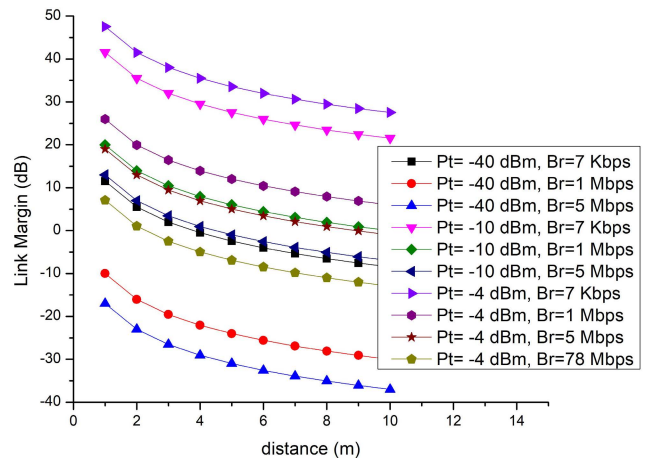
FIGURE 20. Link margin with respect to distance between transmitter and receiver antenna for worst case scenario when antenna gain is −29.5 dB for 3D canonical right arm tissue model.

V. CONCLUSION

In this dissemination, first time design steps and studies on implantable DRA have been presented. The idea of using DRA in biomedical applications was crafted using a rectangular DRA mounted on a PVC substrate. Two design steps were used to construct the implant DRA with dimension 23.5 mm

× 23.5 mm × 5 mm which makes it light and compact to be used in implantable devices. The performance of the proposed DRA was studied in a rectangular single-layer skin phantom, rectangular three-layer (skin-fat-muscle) phantom, cylindrical three-layer (skin-fat-muscle) phantom, and 3D canonical right arm tissue model in the HFSS EM simulator. In all four body models, the proposed DRA shows acceptable performance for the defined 'depth window' and chosen ISM band with a center frequency 2.45 GHz. Further, SAR analysis for acceptable radiation limits was performed and maximum allowable limits as per present international standards were calculated. This study aims to present a strong candidate for DRA in biomedical applications.

REFERENCES

[1] S. Gabriel, R. W. Lau, and C. Gabriel, "The dielectric properties of biological tissues: II. Measurements in the frequency range 10 Hz to 20 GHz," *Phys. Med. Biol.*, vol. 41, no. 11, p. 2251, Nov. 1996. [Online]. Available: http://niremf.ifac.cnr.it/tissprop/

[2] J. Kim and Y. Rahmat-Samii, "Implanted antennas inside a human body: Simulations, designs, and characterizations," *IEEE Trans. Microw. Theory Techn.*, vol. 52, no. 8, pp. 1934–1943, Aug. 2004, doi: 10.1109/TMTT.2004.832018.

[3] A. Kiourti and K. S. Nikita, "A review of implantable patch antennas for biomedical telemetry: Challenges and solutions [wireless corner]," *IEEE Antennas Propag. Mag.*, vol. 54, no. 3, pp. 210–228, Jun. 2012, doi: 10.1109/MAP.2012.6293992.

[4] A. Kiourti and K. S. Nikita, "Miniature scalp-implantable antennas for telemetry in the MICS and ism bands: Design, safety considerations and link budget analysis," *IEEE Trans. Antennas Propag.*, vol. 60, no. 8, pp. 3568–3575, Aug. 2012, doi: 10.1109/TAP.2012.2201078.

[5] A. Kiourti, J. R. Costa, C. A. Fernandes, and K. S. Nikita, "A broadband implantable and a dual-band on-body repeater antenna: Design and transmission performance," *IEEE Trans. Antennas Propag.*, vol. 62, no. 6, pp. 2899–2908, Jun. 2014, doi: 10.1109/TAP.2014.2310749.

[6] A. Kiourti and K. S. Nikita, "Implantable antennas: A tutorial on design, fabrication, and *in vitro/in vivo* testing," *IEEE Microw. Mag.*, vol. 15, no. 4, pp. 77–91, Jun. 2014, doi: 10.1109/MMM.2014.2308765.

[7] Z.-J. Yang, L. Zhu, and S. Xiao, "An implantable circularly polarized patch antenna design for pacemaker monitoring based on quality factor analysis," *IEEE Trans. Antennas Propag.*, vol. 66, no. 10, pp. 5180–5192, Oct. 2018, doi: 10.1109/TAP.2018.2862242.

[8] L. Matekovits, J. Huang, I. Peter, and K. P. Esselle, "Mutual coupling reduction between implanted microstrip antennas on a cylindrical biometallic ground plane," *IEEE Access*, vol. 5, pp. 8804–8811, 2017, doi: 10.1109/ACCESS.2017.2703872.

[9] F. Merli, B. Fuchs, J. R. Mosig, and A. K. Skrivervik, "The effect of insulating layers on the performance of implanted antennas," *IEEE Trans. Antenna Propag.*, vol. 59, no. 1, pp. 21–31, Jan. 2011, doi: 10.1109/TAP.2010.2090465.

[10] A. Kiourti and K. S. Nikita, "A review of in-body biotelemetry devices: Implantables, ingestibles, and injectables," *IEEE Trans. Biomed. Eng.*, vol. 64, no. 7, pp. 1422–1430, Jul. 2017, doi: 10.1109/TBME.2017.2668612.

[11] C. Liu, Y.-X. Guo, and S. Xiao, "Circularly polarized helical antenna for ISM-band ingestible capsule endoscope systems," *IEEE Trans. Antennas Propag.*, vol. 62, no. 12, pp. 6027–6039, Dec. 2014, doi: 10.1109/TAP.2014.2364074.

[12] Z. Duan and L.-J. Xu, "Dual-band implantable antenna with circular polarisation property for ingestible capsule application," *Electron. Lett.*, vol. 53, no. 16, pp. 1090–1092, Aug. 2017, doi: 10.1049/el.2017.1681.

[13] H. Rajagopalan and Y. Rahmat-Samii, "Wireless medical telemetry characterization for ingestible capsule antenna designs," *IEEE Antennas Wireless Propag. Lett.*, vol. 11, pp. 1679–1682, Jan. 2013, doi: 10.1109/LAWP.2013.2238502.

[14] R. Das and H. Yoo, "A wideband circularly polarized conformal endoscopic antenna system for high-speed data transfer," *IEEE Trans. Antennas Propag.*, vol. 65, no. 6, pp. 2816–2826, Jun. 2017, doi: 10.1109/TAP.2017.2694700.

[15] G. A. Conway and W. G. Scanlon, "Antennas for over-body-surface communication at 2.45 GHz," *IEEE Trans. Antennas Propag.*, vol. 57, no. 4, pp. 844–855, Apr. 2009, doi: 10.1109/TAP.2009.2014525.

[16] W. Lei, H. Chu, and Y.-X. Guo, "Design of a circularly polarized ground radiation antenna for biomedical applications," *IEEE Trans. Antennas Propag.*, vol. 64, no. 6, pp. 2535–2540, Jun. 2016, doi: 10.1109/TAP.2016.2552551.

[17] C. Liu, Y.-X. Guo, and S. Xiao, "Capacitively loaded circularly polarized implantable patch antenna for ISM band biomedical applications," *IEEE Trans. Antennas Propag.*, vol. 62, no. 5, pp. 2407–2417, May 2014, doi: 10.1109/TAP.2014.2307341.

[18] C. Liu, Y.-X. Guo, H. Sun, and S. Xiao, "Design and safety considerations of an implantable rectenna for far-field wireless power transfer," *IEEE Trans. Antennas Propag.*, vol. 62, no. 11, pp. 5798–5806, Nov. 2014, doi: 10.1109/TAP.2014.2352363.

[19] Y. Zhang, C. Liu, X. Liu, K. Zhang, and X. Yang, "A wideband circularly polarized implantable antenna for 915 MHz ISM-band biotelemetry devices," *IEEE Antennas Wireless Propag. Lett.*, vol. 17, no. 8, pp. 1473–1477, Aug. 2018, doi: 10.1109/LAWP.2018.2849847.

[20] M. K. Magill, G. A. Conway, and W. G. Scanlon, "Tissue-independent implantable antenna for in-body communications at 2.36–2.5 GHz," *IEEE Trans. Antennas Propag.*, vol. 65, no. 9, pp. 4406–4417, Sep. 2017, doi: 10.1109/TAP.2017.2708119.

[21] J. M. Felicio, J. R. Costa, and C. A. Fernandes, "Dual-band skin-adhesive repeater antenna for continuous body signals monitoring," *IEEE J. Electromagn., RF Microw. Med. Biol.*, vol. 2, no. 1, pp. 25–32, Mar. 2018, doi: 10.1109/JERM.2018.2806186.

[22] I. Gani and H. Yoo, "Multi-band antenna system for skin implant," *IEEE Microw. Wireless Compon. Lett.*, vol. 26, no. 4, pp. 294–296, Apr. 2016, doi: 10.1109/LMWC.2016.2538470.

[23] M. K. Magill, G. A. Conway, and W. G. Scanlon, "Circularly polarized dual-mode wearable implant repeater antenna with enhanced into-body gain," *IEEE Trans. Antennas Propag.*, vol. 68, no. 5, pp. 3515–3524, May 2020, doi: 10.1109/TAP.2020.2972335.

[24] F. Merli, L. Bolomey, J.-F. Zurcher, G. Corradini, E. Meurville, and A. K. Skrivervik, "Design, realization and measurements of a miniature antenna for implantable wireless communication systems," *IEEE Trans. Antennas Propag.*, vol. 59, no. 10, pp. 3544–3555, Oct. 2011, doi: 10.1109/TAP.2011.2163763.

[25] W. Xia, K. Saito, M. Takahashi, and K. Ito, "Performances of an implanted cavity slot antenna embedded in the human arm," *IEEE Trans. Antennas Propag.*, vol. 57, no. 4, pp. 894–899, Apr. 2009, doi: 10.1109/TAP.2009.2014579.

[26] R. Chávez-Santiago, C. Garcia-Pardo, A. Fornes-Leal, A. Vallés-Lluch, G. Vermeeren, W. Joseph, I. Balasingham, and N. Cardona, "Experimental path loss models for in-body communications within 2.36-2.5 GHz," *IEEE J. Biomed. Health Informat.*, vol. 19, no. 3, pp. 930–937, May 2015, doi: 10.1109/JBHI.2015.2418757.

[27] A. Ba, M. Vidojkovic, K. Kanda, N. F. Kiyani, M. Lont, X. Huang, X. Wang, C. Zhou, Y. H. Liu, M. Ding, and B. Büsze, "A 0.33 nJ/bit IEEE802.15.6/proprietary MICS/ISM wireless transceiver with scalable data rate for medical implantable applications," *IEEE J. Biomed. Health Inform.*, vol. 19, no. 3, pp. 920–929, May 2015, doi: 10.1109/JBHI.2015.2414298.

[28] *IEEE Standard for Safety Levels With Respect to Human Exposure to Radio Frequency Electromagnetic Fields, 3 KHz to 300 GHz*, Standard C95.1-1991, 1999.

[29] *IEEE Standard for Safety Levels With Respect to Human Exposure to Radio Frequency Electromagnetic Fields, 3 KHz to 300 GHz*, Standard C95.1-2005, 2005.

[30] *IEEE Standard for Safety Levels With Respect to Human Exposure to Electric, Magnetic, and Electromagnetic Fields, 0 Hz to 300 GHz*, Standard C95.1, 2019.

[31] *ICNIRP Guidelines for Limiting Exposure to Time Varying Electric Field and Magnetic Field*. Accessed: Mar. 9, 2021. [Online]. Available: https://www.icnirp.org/cms/upload/publications/ICNIRPLFgdl.pdf

[32] M. Alizadeh-Osgouei, Y. Li, and C. Wen, "A comprehensive review of biodegradable synthetic polymer-ceramic composites and their manufacture for biomedical applications," *Bioactive Mater.*, vol. 4, pp. 22–36, Dec. 2019, doi: 10.1016/j.bioactmat.2018.11.003.

[33] M. Lungu, L. Moldovan, O. Craciunescu, and C. Doicin, "Biocompatible blends based on polyvinyl chloride and natural polymers for medical device fabrication," *Materiale Plastice*, vol. 47, pp. 278–281, Sep. 2010.

[34] I. Peter and S. S. Singhwal, "5G antenna materials and ensuing challenges," in *5G Antenna Mater. Ensuing Challenges*. Cham, Switzerland: Springer, Jan. 2022, doi: 10.1007/978-3-030-87605-0_11.

[35] Y.-W. Chen, J. Moussi, J. L. Drury, and J. C. Wataha, "Zirconia in biomedical applications," *Expert Rev. Med. Devices*, vol. 13, no. 10, pp. 945–963, Oct. 2016, doi: 10.1080/17434440.2016.1230017.

[36] M. T. Sebastian, R. Ubic, and H. Jantunen, "Low-loss dielectric ceramic materials and their properties," *Int. Mater. Rev.*, vol. 60, no. 7, pp. 392–412, Jul. 2015.

[37] T. Safronova, V. I. Putlayev, A. G. Veresov, A. V. Kuznetsov, M. A. Shekhirev, and K. A. Agahi, "Biocompatible ceramics for implants based on calcium phosphates," *MRS Proc.*, vol. 951, no. 1, pp. 31–36, 2006, doi: 10.1557/PROC-0951-E12-31.

[38] A. Wypych, I. Bobowska, M. Tracz, A. Opasinska, S. Kadlubowski, A. Krzywania-Kaliszewska, J. Grobelny, and P. Wojciechowski, "Dielectric properties and characterisation of titanium dioxide obtained by different chemistry methods," *J. Nanomater.*, vol. 2014, pp. 1–9, Mar. 2014, doi: 10.1155/2014/124814.

[39] I. Sailer, A. Philipp, A. Zembic, B. E. Pjetursson, C. H. F. Hämmerle, and M. Zwahlen, "A systematic review of the performance of ceramic and metal implant abutments supporting fixed implant reconstructions," *Clin. Oral Implants Res.*, vol. 20, pp. 4–31, Sep. 2009, doi: 10.1111/j.1600-0501.2009.01787.x.

[40] J. Han, J. Zhao, and Z. Shen, "Zirconia ceramics in metal-free implant dentistry," Advances in Applied Ceramics, vol. 116, pp. 138-150, Apr. 2017, doi: 10.1080/17436753.2016.1264537.

[41] *American Ceramic Society Website*. Accessed: Feb. 2, 2021. [Online]. Available: http://ceramics.org/wp-content/bulletin/2019/pdf/August2019.pdf

[42] *Laird Website*. Accessed: Feb. 9, 2021. [Online]. Available: https://www.laird.com/products/

[43] *Skyworks Website*. Accessed: Feb. 9, 2021. [Online]. Available: https://cm-sitecore.skyworksinc.com

[44] *Maruwa Website*. Accessed: Feb. 9, 2021. [Online]. Available: https://www.maruwa-g.com/e/products/ceramic/powdery-molding-goods-1.html

[45] *Preperm Website*. Accessed: Feb. 9, 2021. [Online]. Available: https://www.preperm.com/products/

[46] E. A. J. Marcatili, "Dielectric rectangular waveguide and directional coupler for integrated optics," *Bell Syst. Tech. J.*, vol. 48, no. 7, pp. 2071–2102, Sep. 1969.

[47] R. K. Mongia and P. Bhartia, "Dielectric resonator antennas—A review and general design relations for resonant frequency and bandwidth," *Int. J. Microw. Millim.-Wave Comput.-Aided Eng.*, vol. 4, no. 3, pp. 230–247, Jul. 1994.

[48] R. K. Mongia and A. Ittipiboon, "Theoretical and experimental investigations on rectangular dielectric resonator antennas," *IEEE Antennas Propag.*, vol. 45, no. 9, pp. 1348–1356, Sep. 1997.

[49] M. S. Islam, K. P. Esselle, D. Bull, and P. M. Pilowsky, "Converting a wireless biotelemetry system to an implantable system through antenna redesign," *IEEE Trans. Microw. Theory Techn.*, vol. 62, no. 9, pp. 1890–1897, Sep. 2014, doi: 10.1109/TMTT.2014.2342665.

[50] K. Bazaka and M. V. Jacob, "Implantable devices: Issues and challenges," *Electronics*, vol. 2, no. 1, pp. 1–34, 2013, doi: 10.3390/electronics2010001.

[51] L. Matekovits, Y. Su, and I. Peter, "On the radiation mechanism of implanted antennas with large conformal ground plane," *IET Microw., Antennas Propag.*, vol. 11, no. 12, pp. 1765–1769, Sep. 2017, doi: 10.1049/iet-map.2017.0280.

SUMER SINGH SINGHWAL (Member, IEEE) received the Bachelor of Engineering degree from M. D. University Rohtak, in 2003, the master's degree in engineering from the Birla Institute of Technology Mesra, Ranchi, in 2012, and the Ph.D. degree in electronics and communication engineering from Uttarakhand Technical University, Dehradun, in 2020. He worked as a Postdoctoral Researcher with the Poitecnico di Torino, Italy, from 2020 to 2021, where he is currently a Honorary Research Fellow with the Department of Electronics and Telecommunication. He has been working in the field of dielectric resonator antennas for different wireless applications. He is also working as an Assistant Professor with the Department of Electronics and Communication Engineering, Chandigarh University, Chandigarh, India. He has published/presented several papers in refereed journals and conferences. He has also written a book chapter in Springer series. His research interests include dielectric resonator antennas, MIMO DRA, body implantable antennas, and tunable DRA. He is a reviewer of several journals of international repute, such as *IET Microwaves, Antennas & Propagation*, IEEE ANTENNAS AND WIRELESS PROPAGATION LETTERS, *IETE Technical Review*, and *AEU—International Journal of Electronics and Communication*.

LADISLAU MATEKOVITS (Senior Member, IEEE) received the degree in electronic engineering from the Institutul Politehnic din Bucureti, Bucureti, Romania, in 1992, and the Ph.D. degree (Dottorato di Ricerca) in electronic engineering from the Politecnico di Torino, Torino, Italy, in 1995.

He joined the Department of Electronics and Telecommunications as an Assistant Professor, in 2002. He was appointed as a Senior Assistant Professor, in 2005, and an Associate Professor, in 2014. In February 2017, he obtained a Full Professor qualification. Italy. In late 2005, he was a Visiting Scientist with the Antennas and Scattering Department, FGAN-FHR (now Fraunhofer Institute), Wachtberg, Germany. Beginning July 2009, for two years, he has been a Marie Curie Fellow at Macquarie University, Sydney, NSW, Australia, where he also held a visiting academic position, in 2013, and in 2014, has been appointed as a Honorary Fellow. Since 1995, he has been with the Department of Electronics and Telecommunications, Politecnico di Torino, first with a Postdoctoral Fellowship and then as a Research Assistant. Since 2020, he has been an Honorary Professor with the Polytechnic University of Timisoara, Romania, and an Associate of the Italian National Research Council. He has been appointed as a member of the National Council for the Attestation, University Degrees, Diplomas and Certificates (CNATDCU), Romania, for the term 2020–2024. He has published more than 375 articles, including more than 100 journal contributions. His research interests include numerical analysis of printed antennas and in particular development of new, numerically efficient full-wave techniques to analyze large arrays, and active and passive metamaterials for cloaking applications. Material parameter retrieval of these structures by inverse methods and different optimization techniques has also been considered. In the last years, bio-electromagnetic aspects have also been contemplated, as, for example, design of implantable antennas or development of nano-antennas, for example, for drug delivery applications. He has delivered seminars on these topics all around the world: Europe, USA (AFRL/MIT-Boston), Australia, China, and Russia. He has been invited to serve as a Research Grant Assessor for government funding calls (Romania, Italy, Croatia, and Kazakhstan) and an International Expert in Ph.D. thesis evaluation by several universities from Australia, India, Pakistan, and Spain.

Prof. Matekovits has been a member of the Organizing Committee of the International Conference on Electromagnetics in Advanced Applications (ICEAA), since 2010, and he is a member of the technical program committees of several conferences. He was a recipient of various awards in international conferences, including the 1998 URSI Young Scientist Award (Thessaloniki, Greece), the Barzilai Award 1998 (Young Scientist Award, granted every two years by the Italian National Electromagnetic Group), and the Best AP2000 Oral Paper on Antennas, ESA-EUREL Millennium Conference on Antennas and Propagation (Davos, Switzerland). He was also a recipient of the Motohisa Kanda Award 2018, for the most cited paper of the IEEE TRANSACTIONS ON ELECTROMAGNETIC COMPATIBILITY in the past five years. More recently, he has been awarded with the 2019 American Romanian Academy of Arts and Sciences (ARA) Medal of Excellence in Science and the Ad Astra Award 2020, as a Senior Researcher for Excellence in Research. He has been an Assistant Chairperson and the Publication Chairperson of the European Microwave Week 2002, (Milan, Italy, and the General Chair of the 11th International Conference on Body Area Networks (BodyNets), in 2016. He serves as an Associate Editor for IEEE ACCESS, IEEE ANTENNAS AND WIRELESS PROPAGATION LETTERS, and *IET MAP*, and a reviewer for different journals.

ILDIKO PETER received the M.S. degree in bio-chemistry from the Università degli Studi di Torino, and the Ph.D. degree in material science and engineering from the Politecnico di Torino, Italy. In 2018, she has acquired the "Habilitation for Full Professor" in the field of materials engineering. She has been a Visiting Researcher with Macquarie University, Sydney, NSW, Australia, since 2010, and a Visiting Professor with Universitatea Politecnica Timisoara, Romania, from 2015 to 2018. Since 2018, she has been a member of the Doctoral School, Universitatea Valahia Targoviste, Romania. She is currently an Associate Professor with the Department of Industrial Engineering and Management, University of Medicine, Pharmacy, Science and Technology "George Emil Palade" Targu Mures, Romania. She has more than 150 publications and has delivered more than ten invited talks. Her research activity is highly interdisciplinary involving different people, departments, and research centres at local, national, and international level. Her research interests include development and characterization of different metallic alloys for automotive/aeronautical industries and biomedical applications, the development, optimization and characterization of thin and thick coatings on metallic substrates, the study of metal-based alloy nanoparticles for oxygen reduction reaction, the development and characterization of metals containing humidity sensors for environmental monitoring, the synthesis and characterization of materials for advanced electromagnetic applications, and synthesis and characterization of piezoelectric ceramic materials. She is the co-inventor of two granted patents. She has participated in various European and national projects. She is a member of the American Romanian Academy of Arts and Science, Asociazione Italiana di Metallurgia, and the Consorzio Interuniversitario Nazionale per la Scienza e Tecnologia dei Materiali. She is acting as a reviewer for several journals, and since 2015, she has been serving as an Associate Editor for IEEE Access, a Guest Editor for *Metals*, Special Issue "Development of Metallic Materials Through Hot or Cold Processes and Characterization of the Metallic Alloys," and a Topic Editor for *Metals*, since 2020. She has been an Editorial Board Member of *Open Access Journal of Engineering Sciences*, since 2020, a Managing Editor of *Acta Marisiensis: Seria Technologica*—the journal of the George Emil Palade University of Medicine, Pharmacy, Sciences, and Technology of Targu Mures. She has been invited to serve as a Research Grant Assessor for government funding calls in Romania.

BINOD KUMAR KANAUJIA (Senior Member, IEEE) received the B.Tech. degree in electronics engineering from KNIT Sultanpur, India, in 1994, and the M.Tech. and Ph.D. degrees from the Department of Electronics Engineering, Indian Institute of Technology Banaras Hindu University, Varanasi, India, in 1998 and 2004, respectively. He was a Lecturer, from 1996 to 2005, and a Reader, from 2005 to 2008, with the Department of Electronics & Communication Engineering, and also the Head of the Department of M. J.P. Rohilkhand University, Bareilly, India. Prior to his career in academics, he had worked as an Executive Engineer with the Research and Development Division, M/s UPTRON India Ltd. He has been working as a Professor with the School of Computational and Integrative Sciences, Jawaharlal Nehru University, New Delhi, since August 2016. Before joining Jawaharlal Nehru University, he had been with the Department of Electronics & Communication Engineering, Ambedkar Institute of Advanced Communication Technologies & Research (formerly the Ambedkar Institute of Technology), Delhi, as a Professor, since February 2011, and was an Associate Professor, from 2008 to 2011. He has been credited to publish more than 353 research papers with more than 3184 citations with an H-index of 26 in peer-reviewed journals and conferences. He had supervised 70 M.Tech. and 25 Ph.D. research scholars in the field of microwave engineering. His research interests include design and modeling of microstrip antenna, dielectric resonator antenna, left-handed metamaterial microstrip antenna, shorted microstrip antenna, ultra wideband antennas, reconfigurable, and circular polarized antenna for wireless communication. He is a reviewer of several journals of international repute, such as *IET Microwaves, Antennas & Propagation*, IEEE Antennas and Wireless Propagation Letters, *Wireless Personal Communications*, *Journal of Electromagnetic Wave and Application*, *Indian Journal of Radio and Space Physics*, *IETE Technical Review*, *International Journal of Electronics*, *International Journal of Engineering Science*, IEEE Transactions on Antennas and Propagation, *AEU—International Journal of Electronics and Communication*, and *International Journal of Microwave and Wireless Technologies*. He has been awarded a Junior Research Fellowship by UGC Delhi, for his outstanding work in electronics field, in 2001 and 2002. He had successfully executed four research projects sponsored by several agencies of the Government of India, such as DRDO, DST, AICTE, and ISRO. He is also a member of several academic and professional bodies, such as IEEE, Institution of Engineers (India), Indian Society for Technical Education, and The Institute of Electronics and Telecommunication Engineers of India.

● ● ●